Int. J. Electrochem. Sci., 15 **(2020)** 6620 – 6628, doi: 10.20964/2020.07.36

International Journal of
ELECTROCHEMICAL
SCIENCE
www.electrochemsci.org

Short Communication

Simultaneous Detection of Hydroquinone and Catechol at a Three-Dimensional Graphene-Modified Glassy Carbon Electrode

Yuting Wang, Xiangfei Chen, Dejuan Huang[*] *, Tianxiang Jin*[*]

Jiangxi Province Key Laboratory of Polymer Micro/Nano Manufacturing and Devices, East China University of Technology, Nanchang, Jiangxi, 330013, China.
[*]E-mail: 201660027@ecut.edu.cn (T. Jin) djhuang@ecut.edu.cn (D. Huang)

Received: 17 January 2020 / *Accepted:* 29 April 2020 / *Published:* 10 June 2020

Three-dimensional graphene (3DG) is presented as an excellent electrocatalyst for the simultaneous detection of hydroquinone (HQ) and catechol (CC) by cyclic voltammetry (CV) and differential pulse voltammetry (DPV). Morphology and structure of 3DG were characterized by scanning electron microscopy (SEM), X-ray diffraction (XRD), and X-ray photoelectron spectroscopy (XPS). Compared with the bare glassy carbon electrode (GCE), the 3DG-modified GCE exhibits better electrocatalytic activity in the redox reaction of HQ and CC. The 3DG-modified GCE detects both isomers selectively and sensitively by DPV and CV, latter showing a peak-to-peak separation of 190 mV. The detection limits for HQ and CC can reach 0.35 and 0.6 μM (S/N = 3), respectively, with wide linear ranges of 1–1000 μM in the presence of 50 μM of the respective other isomer. This work provides a strategy for the development of high-performance electrochemical sensors.

Keywords: Three-dimensional graphene; Electrochemical sensor; Simultaneous detection; Hydroquinone; Catechol

1. INTRODUCTION

Hydroquinone (HQ) and catechol (CC) are two dihydroxybenzene isomers that are widely used in the chemical industry. HQ is used in the synthesis of photographic developers, dyestuffs, antioxidants, etc., while catechol is commonly used in the synthesis of pesticides, perfumes, resins, coatings, etc. [1] However, both isomers are toxic to humans and present a great threat to the surrounding environment. [2] Therefore, developing an effective method for the easy detection of HQ and CC is of high importance. However, the usual coexistence of the chemically similar isomers makes their direct, simultaneous, and specific measurement difficult. [3, 4] In recent years, different techniques have been applied to detect dihydroxybenzene isomers, including fluorescence

spectroscopy, spectrophotometry, chemiluminescence, capillary electrochromatography, as well as electrochemical methods. [5, 6] Among these methods, electrochemical detection is sensitive, stable and accurate [7-12] and has been widely used in electrochemical capacitors [13, 14], biosensors [15-18], fuel cells [7], and electrocatalysis [19, 20]. Therefore, electrochemical detection is a highly promising analytical technique for a wide range of applications.

Superior analytical performances have been reported for glassy carbon electrodes modified with various nanomaterials or quantum dots, such as ZnS/NiS@ZnS quantum dots [21], multi-walled carbon nanotubes/polydopamine/gold nanoparticle composites [22], and Au-Pd nanoflower/reduced graphene oxide nanocomposites [23]. These materials have been explored as electrochemical for the direct and simultaneous detection of HQ and CC. However, reported methods for fabricating these materials are generally complex, expensive and highly toxic, which are thus not suitable for the large-scale fabrication in the chemical industry.

In this regard, we focused on three-dimensional graphene (3DG), which has been reported to exhibit excellent electronic, and mechanical properties [24]. Furthermore, the fast electron transfer process [25] and extremely large surface area of 3DG promise a high electrochemical reaction rate [26]. 3DG even maintains the bioactivity because of its high specific surface area and good biocompatibility [27].

Therefore, we developed a simple and environment-friendly approach to fabricate 3DG. Subsequently, the 3DG modified glassy carbon electrode (3DG@GCE) was applied as an electrochemical sensor to determine the HQ and CC content. The results showed that 3DG substantially improved the electrochemical performance of the glassy carbon electrode, and the as-prepared electrochemical sensor was successfully applied to simultaneously detect HQ and CC, exhibiting a large detection range, low detection limit, high sensitivity, and good selectivity.

2. EXPERIMENTAL SECTION

2.1 Materials

$KMnO_4$, KOH, $NaNO_3$, 98% H_2SO_4, 30% H_2O_2, and graphite powder of analytical grade were purchased from Aladdin Reagent Co., Ltd. (China) and used as received without further purification.

2.2 Preparation of 3DG

Graphene oxides (GOs) were prepared by a modified Hummers method, similar to the method described in our previous work [25]. Therefore, 45 mL GO suspension (2 mg/mL) was freeze dried for 40 h to obtain three-dimensional graphene aerogels, denoted as 3DG.

2.3 Preparation of modified electrodes

GCE (φ=3 mm, diameter) was sequentially polished with 0.3, and 0.05 μm alumina powders and then washed ultrasonically with water and then ethanol for several minutes. The cleaned GCE was

dried with nitrogen steam. The 3DG@GCE was fabricated by drop-casting 20 μL of 3DG/N, N-dimethyl formamide (3DG-DMF) suspension (2 mg/L) on the GCE surface, following by drying with an infrared lamp.

2.4 Material characterization

SEM imaging was performed by a field emission scanning electron microscope (FE–SEM, Hitachi S–4800) at 10 kV. The material's structure was investigated by XRD analysis (Shimadzu, X–6000, Cu Kα radiation). The specific surface area (SSA) of the UGA and FGA was examined by N_2 adsorption/desorption using the BET method. XPS measurements were performed on a Thermo Fisher X-ray photoelectron spectrometer with Al Kα radiation and a chamber pressure of 5×10^{-9} Torr (analysis spot size diameter, 400 μm).

2.5 Electrochemical measurements

A three-electrode system was applied to analyze the electrochemical properties of the samples. All the electrochemical measurements were carried out on a CHI 660E electrochemical workstation using 0.10 mol/L PBS solution (pH=3.0) as electrolyte. As working electrode, either a bare GCE or the 3DG@GCE was used. A saturated calomel electrode (SCE) and Pt wire were used as the reference and counter electrode, respectively. The electrochemical properties of the bare GCE and 3DG@GCE were analyzed by CV and DPV.

3. RESULTS AND DISCUSSION

3.1. Characterization of 3DG

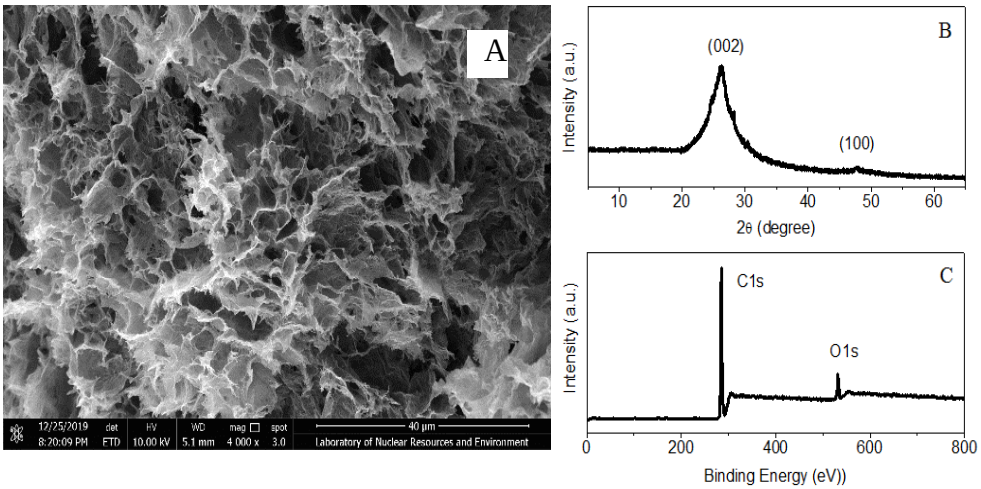

Figure 1. (A) SEM image, (B) XRD pattern, and (C) XPS spectrum of the as-prepared 3DG.

The microscopic structure of as-prepared 3DG was characterized by SEM (Figure 1A),

revealing a porous network structure with a uniform pore size of 50 nm. The three-dimensional structure of 3DG was highly interconnected, and the graphene sheets were well dispersed without aggregations.

XRD was performed to characterize the crystallographic structure of 3DG (Figure 1B). The typical peaks at around 26.2° and 48.0° were indexed to the (002) and (100) crystal planes of the graphite structure, respectively [28]. This result shows that graphene oxide was effectively reduced, ensuring high conductivity of the 3DG material.

XPS was utilized to further investigate the chemical composition of 3DG. The XPS spectrum (Figure 1C) of 3DG exhibits two peaks at 285 and 532 eV, corresponding to C1s and O1s, respectively [29]. The O1s peak of 3DG is very small, suggesting that the oxygen-containing functional groups of GO were partially eliminated during the fabrication, which is beneficial to the redox reaction.

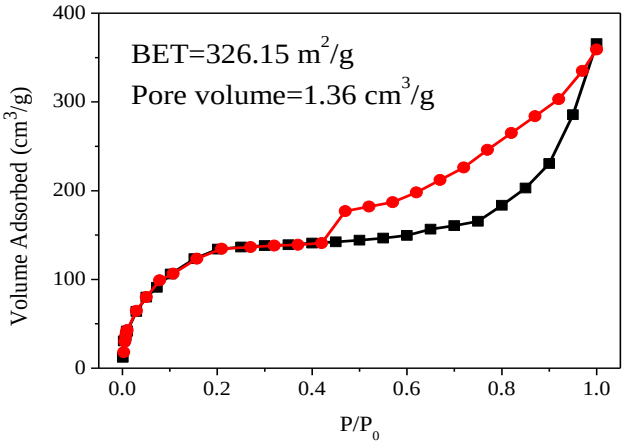

Figure 2. N_2 adsorption-desorption isotherms of 3DG

The Brunauer-Emmett-Teller (BET) surface area of 3DG was investigated by a nitrogen adsorption-desorption measurement (Figure. 2), revealing a type IV isotherm. The 3DG adsorption curve increased significantly in the relative pressure (P/P_0) range of 0.4–0.8, indicating a large number of mesopores. The sharp increase of adsorbed N_2 at $P/P_0 > 0.8$ could be ascribed to the adsorption of N_2 in large-size pores. The BET analysis revealed for 3DG a specific surface area of 326.15 m^2/g with a total pore volume of 1.36 cm^3 /g. This large specific surface area offers abundant electrochemically active sites, which can adsorb more analyte molecules for the electrochemical reaction. The hierarchical pore structure of 3DG is also instrumental in the rapid diffusion of analyte molecules, which further enhances the electrocatalytic activity.

3.2. Electrochemical behavior of 3DG modified electrode

The CV curves of solutions of HQ and CC using either the bare GCE or the 3DG@GCE as working electrode are presented in Figure 2A, B. At the bare GCE, the oxidation/reduction peaks of HQ and CC appeared at 0.145/0.012 V and 0.385/0.015 V, respectively.

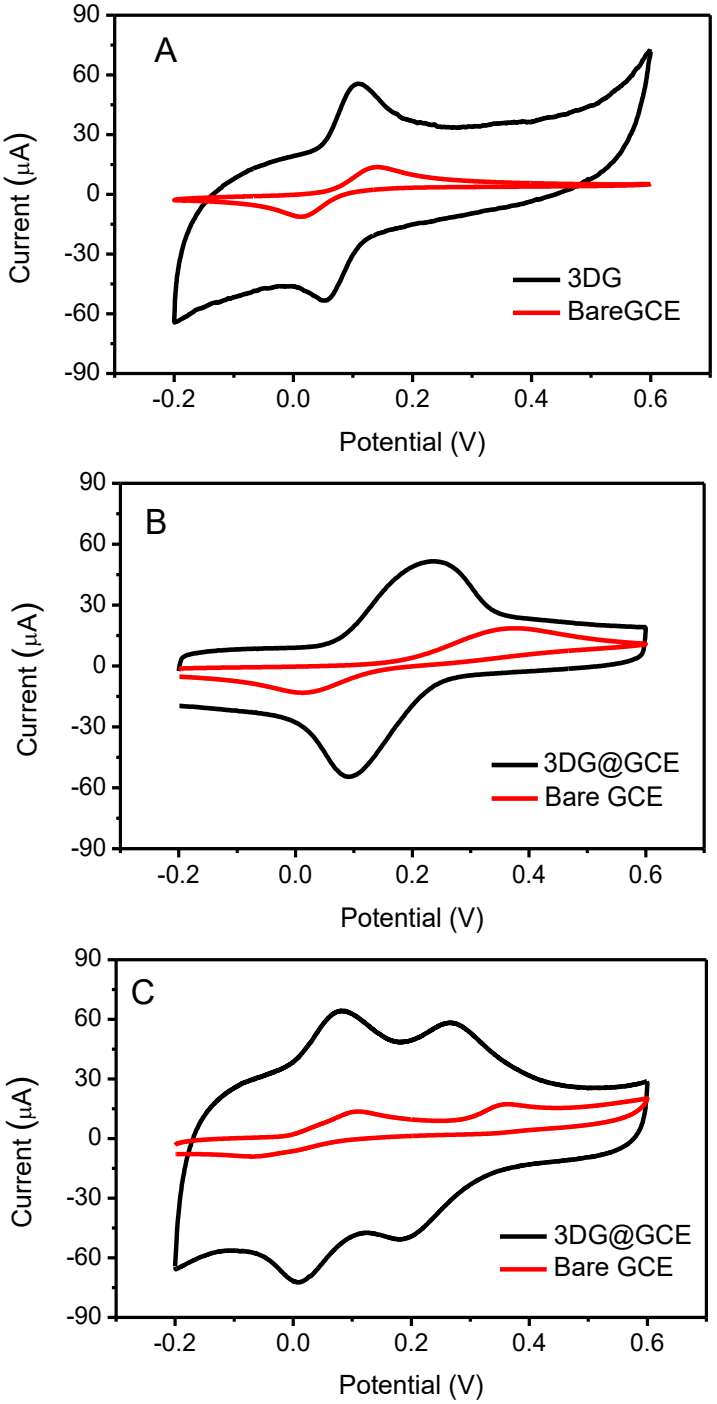

Figure 3. CV curves of 3DG@GCE and bare GCE in the presence of (A) 0.3 mM HQ, (B) 0.3 mM CC, and (C) a mixed solution of 0.3 mM HQ and 0.3 mM CC at a scan rate of 100 mV/s in 0.1 mol/L PBS (pH = 3.0)

The corresponding oxidation/reduction peak potential separations of HQ and CC were 133 and 370 mV, respectively. In contrast, at the 3DG@GCE, the oxidation/reduction peaks of HQ and CC were observed at 0.109/0.053 V and 0.255/0.095 V, respectively. The corresponding oxidation/reduction peak potential separations of HQ and CC were 56 and 160 mV, respectively. The significantly smaller peak potential separations measured with the 3DG@GCE compared with the bare

GCE suggest a much faster electron transfer at the 3DG@GCE. Furthermore, significantly larger HQ and CC peak currents were measured with the 3DG@GCE than with the bare GCE. These data prove that the overpotential of the redox reactions of HQ and CC is significantly smaller on the 3DG@GCE than on the bare GCE, ensuring a better electrochemical reversibility.

The CV curves of a mixed solution of HQ and CC recorded on the GCE and 3DG@GCE are shown in Figure 2C. Two weak oxidation peaks are observed on the bare GCE, and the peak potentials could not be accurately distinguished. In comparison, for the 3DG@GCE, two apparent oxidation peaks are observed at 0.095 and 0.285 V for HQ and CC, respectively. The corresponding peak potential difference between HQ and CC was 190 mV. Moreover, the reduction peaks of CC and HQ are also clearly distinguished at the 3DG@GCE. This excellent performance is due to the large electroactive surface area and high electrical conductivity of the 3DG material. The probable electrode reactions for HQ and CC are as follows. The two oxygen-hydrogen bonds of phenolic hydroxyl groups broke. In the meantime, HQ and CC lost two protons and two electrons and transformed into the corresponding quinonoid structure [30, 31].

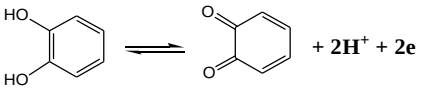

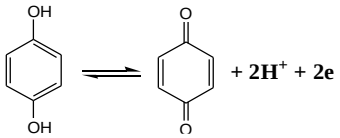

3.3. Determination of HQ and CC with the 3DG@GCE

The practical performance of the 3DG@GCE was evaluated in a DPV study, which was conducted for different concentrations of one analyte in the presence of the other analyte at a constant concentration. As presented in Figure 4A, the HQ oxidation current increased with increasing HQ concentration, while the oxidation peak potential remained unchanged.

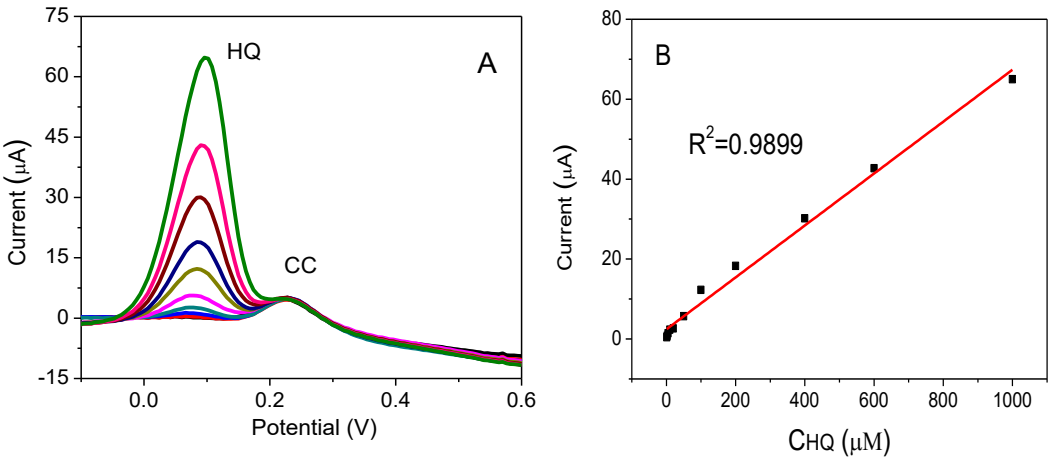

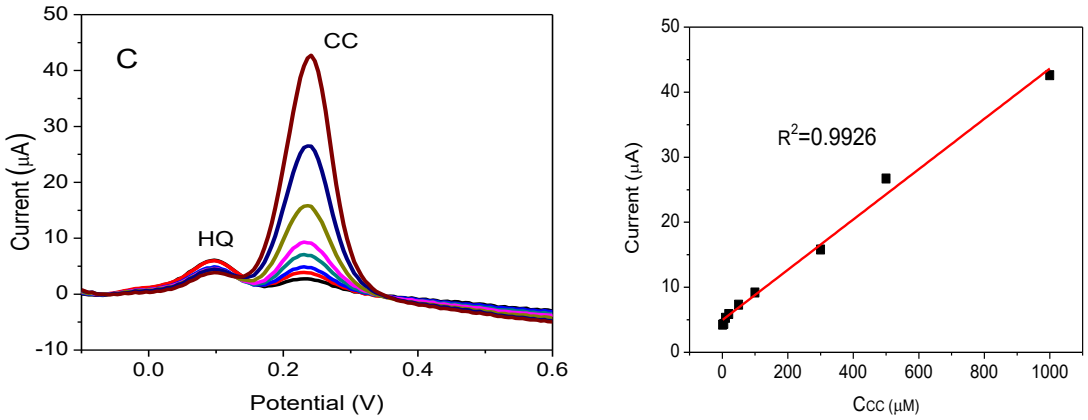

Figure 4. (A) DPV curves of 50 μM CC and HQ at different concentrations; (B) calibration plot for current response vs. the concentration of HQ; (C) DPV curves of 50 μM HQ and different concentrations of CC; (D) calibration plot for current response vs. CC concentration.

Table 1. Comparison of the analytical characteristics of carbon-based material sensors for simultaneous determination of HQ and CC

Electrode	Linear range (μM)		Detection limit (μM)		Ref.
	HQ	CC	HQ	CC	
SWCNT/GCE	0.4–10	0.4–10	0.26	0.12	[32]
MWCNTs/GCE	2.0–100	2.0–100	0.6	0.6	[33]
Au-PdNF/rGO/GCE	1.6–10	2.5–100	0.5	0.8	[34]
TiO_2/C900/GCE	5–300	5–300	1.24	2.05	[35]
C-ZIF-67/PAN-800/GCE	1–120	1–200	1.0	1.0	[36]
NiO/CNT/GCE	10–500	10–400	2.5	2.5	[37]
Au/Fe_3O_4-APTES-GO/GCE	3–137	2–145	1.1	0.8	[38]
Boron-doped graphene/GCE	5–100	1–75	1.6	0.3	[39]
CNCs-RGO/GCE	1–300	1–400	0.87	0.4	[40]
3DG@GCE	1-1000	1-1000	0.35	0.6	This work

SWCNT: single-wall carbon nanotube; MWCNTs: multi-wall carbon nanotube; Au–PdNF/rGO: Au–Pd nanoflower/reduced graphene oxide; NiO/CNT: nickel oxide/carbon nanotube; nanocomposites; APTES: 3-aminopropyl triethoxysilane; AuNPs/Fe_3O_4-APTES–GO: Fe_3O_4-functionalized graphene oxide-gold nanoparticle composite; CNCs–RGO: carbon nanocages-reduced graphene oxide composites.

The detection limit of HQ is about 0.35 μM (S/N = 3). During these measurements, the concentration of CC was constant, and the change in the CC oxidation current was negligible. As depicted in Figure 4B, the HQ peak current increases linearly with the HQ concentration in the range

of 1–1000 לM (R^2 = 0.9899). Figure 4C, D presents the corresponding DPV measurements where the CC concentration is increased, while the HQ concentration is constant. The detection limit of CC is 0.6 לM (S/N = 3). Similarly, the oxidation current of CC is proportional to its concentration in the range of 1–1000 לM (R^2 = 0.9926), and the oxidation current of HQ is not affected by changes in the CC content. These data manifested that HQ and CC oxidation at the 3DG@GCE are independent, which allows the simultaneous detection of both HQ and CC without interference. Furthermore, our results demonstrate that the 3DG@GCE has a high sensitivity and a wide linearity range.

Table 1 shows a comparison of the 3DG@GCE with GCEs modified with other carbon-based materials for the determination of HQ and CC reported in previous studies [32–40], indicating that the 3DG@GCE sensor has higher sensitivities and lower detection limits than the reported GCEs. The excellent performance of the 3DG@GCE can be attributed to the following reasons: (1) the interconnected hierarchical porous architecture not only contributes to the high surface area (326.15 m^2/g) but also promotes massive ion transport (the pore volume: 1.36 cm^3 /g), which makes the electrode/electrolyte interface easily accessible and increases the electrocatalytic efficiency of the redox reaction of the two isomers; (2) 3DG has excellent electronic conductivity and advantageous electrolyte infiltration, which improves the electron transfer rate.

4. CONCLUSION

3DG was prepared by an efficient synthesis method. The fabricated 3DG electrode exhibits a large surface area with a remarkable electrocatalytic activity with good selectivity, promising linearity, and sensitivity for simultaneously detecting HQ and CC in a wide concentration range. As a high-performance sensing material, 3DG may be suitable for large-scale application in chemical industry.

ACKNOWLEDGMENTS
The authors are grateful for the financial support of the National Natural Science Foundation of China (No. 41361088, 41867063) and Foundation of East China University of Technology under Grant No. DHBK2016110.

References

1. C. Ge, H. Li, M. Li, C. Li, X. Wu, B. Yang, *Carbon*, 95 (2015) 1.
2. Y. Zhang, R. Sun, B. Luo, L. Wang, *Electrochim. Acta*, 156 (2015) 228.
3. D. Song, J. Xia, F. Zhang, S. Bi, W. Xiang, Z. Wang, L. Xia, Y. Xia, Y. Li, L. Xia, *Sens. Actuators B: Chem.*, 206 (2015) 111.
4. H. Wei, X.-S. Wu, G.-Y. Wen, Y. Qiao, *Molecules*, 21 (2016) 617.
5. S. Meng, Y. Hong, Z. Dai, W. Huang, X. Dong, *ACS Appl. Mater. & Inter.*, 9 (2017) 12453.
6. H. Zhang, X. Bo, L. Guo, *Sens. Actuators B: Chem.*, 220 (2015) 919.
7. P. Gai, C. Gu, T. Hou, F. Li, *Anal. Chem.*, 89 (2017) 2163.
8. Y. Qian, D. Tang, L. Du, Y. Zhang, L. Zhang, F. Gao, *Biosens. Bioelectron.*, 64 (2015) 177.
9. C. Wang, Y. Qian, Y. Zhang, S. Meng, S. Wang, Y. Li, F. Gao, *Sens. Actuators B: Chem.*, 238 (2017) 434.

10. Y. Qian, T. Fan, P. Wang, X. Zhang, J. Luo, F. Zhou, Y. Yao, X. Liao, Y. Li, F. Gao, *Sens. Actuators B: Chem.*, 248 (2017) 187.
11. Y. Qian, C. Wang, F. Gao, *Anal. Chim. Acta*, 845 (2014) 1.
12. Y. Qian, C. Wang, F. Gao, *Talanta*, 130 (2014) 33.
13. J.F. Chen, T. Zhu, X.P. Fu, G.Y. Ren, C.Y. Wang, *Int. J. Electrochem. Sci.*, 14 (2019) 7293.
14. H.C. Deng, T. Jin, C. Cheng, J. Zheng, Y. Qian, *Int. J. Electrochem. Sci*., 15 (2020) 16 .
15. Y. Qian, C. Wang, F. Gao, *Biosens. Bioelectron.*, 63 (2015) 425.
16. Y. Qian, F. Gao, L. Du, Y. Zhang, D. Tang, D. Yang, *Biosens. Bioelectron*., 74 (2015) 483.
17. T.T. Fan, Y. Du, Y. Yao, J. Wu, S. Meng, J.J. Luo, X. Zhang, D.Z. Yang, C.Y. Wang, Y. Qian, F.L. Gao, *Sens. Actuators B: Chem*., 266 (2018) 9.
18. F. Gao, Y. Qian, L. Zhang, S. Dai, Y. Lan, Y. Zhang, L.L. Du, D. Tang, *Biosens. Bioelectron*., 71 (2015) 158.
19. M. Zhu, Q. Shao, Y. Pi, J. Guo, B. Huang, Y. Qian, X. Huang, *Small*, 13 (2017) 1701295.
20. T. Zhu, J.B. Ding, Q. Shao, Y. Qian, X.Q. Huang, *Chemcatchem*, 11 (2019) 689.
21. Y. Wang, J. Qu, S. Li, Y. Dong, J. Qu, *Microchim. Acta*, 182 (2015) 2277.
22. Y. Wang, Y. Xiong, J. Qu, J. Qu, S. Li, *Sens. Actuators B: Chem*., 223 (2016) 501.
23. Y. Chen, X. Liu, S. Zhang, L. Yang, M. Liu, Y. Zhang, S. Yao, *Electrochim. Acta*, 231 (2017) 677.
24. R. Chen, J. Yan, Y. Liu, J. Li, *J. Phys. Chem*. C, 119 (2015) 8032.
25. Y. Liu, H. Ma, J. Gao, D. Wu, X. Ren, T. Yan, X. Pang, Q. Wei, *Biosens. Bioelectron.*, 79 (2016) 71.
26. W. Sun, F. Hou, S. Gong, L. Han, W. Wang, F. Shi, J. Xi, X. Wang, G. Li, *Sens. Actuators B: Chem.*, 219 (2015) 331.
27. N. Hao, X. Zhang, Z. Zhou, J. Qian, Q. Liu, S. Chen, Y. Zhang, K. Wang, *Sens. Actuators B: Chem.*, 250 (2017) 476.
28. W. Su, W. Feng, Y. Cao, L. Chen, M. Li, C. Song, *Int. J. Electrochem. Sci.*, 13 (2018) 6005.
29. Y. Qian, Y. Lan, J. Xu, F. Ye, S. Dai, *Applied Surface Science* 314 (2014) 991.
30. J.S. Wang, J. Yang, P. Xu, H. Liu, L.L. Zhang, S.H. Zhang, L. Tian, *Sens. Actuators B: Chem.*, 306 (2020) 127590.
31. L. Huang, Y. Cao, D. Diao, *Sens. Actuators B: Chem.*, 305 (2020) 127495.
32. Z. Wang, S. Li, Q. Lv, *Sens. Actuators B: Chem.*, 127 (2007) 420.
33. Y.P. Ding, W.L. Liu, Q.S. Wu, X.G. Wang, Y.P. Ding, W.L. Liu, Q.S. Wu, X.G. Wang, *J. Electroanal. Chem.*, 575 (2005) 275.
34. Y. Chen, X.Y. Liu, S. Zhang, L.Q. Yang, M.L. Liu, Y.Y. Zhang, S.Z. Yao, *Electrochimica Acta*, 231 (2017) 677.
35. Z.Y. Wang, M.S. Li, Y.X. Ye, Y.S. Yang, Y.Q. Lu, X.L. Ma, Z.J. Zhang, X.C. Xiang, *J. Solid State Electrochem.*, 23 (2018) 81.
36. M.X. Zhang, M.S. Li, W.G. Wu, J.K. Chen, X.L. Ma, Z.J. Zhang, X.C. Xiang, *New J. Chem.*, 43 (2019) 3913.
37. L. Zhao, J. Yu, S. Yue, L. Zhang, Z. Wang, P. Guo, Q. Liu, *J. Electroanal. Chem.*, 808 (2018) 245.
38. S. Erogul, S.Z. Bas, M. Ozmen, S. Yildiz, *Electrochim. Acta.*, 186 (2015) 302.
39. Y. Zhang, R. Sun, B. Luo, L. Wang, *Electrochim. Acta.*, 156 (2015) 228.
40. Y.H. Huang, J.H. Chen, X. Sun, Z.B. Su, H.T. Xing, S.R. Hu, W. Weng, H. Xu Guo, W.B. Wu, Y.S. He, *Sens. Actuators B: Chem.*, 212 (2015) 165.